

SGN – Assignment #2

Fernando Aranda Romero, 10882032

Disclaimer: The story plot contained in the following three exercises is entirely fictional.

Exercise 1: Uncertainty propagation

The Prototype Research Instruments and Space Mission Technology Advancement (PRISMA) is a technology in-orbit test-bed mission for demonstrating Formation Flying (FF) and rendezvous technologies, as well as flight testing of new sensors and actuator equipment. It was launched on June 15, 2010, and it involves two satellites: Mango (Satellite 1, ID 36599), the chaser, and Tango (Satellite 2, ID 36827), the target.

You have been provided with an estimate of the states of Satellites 1 and 2 at the separation epoch $t_{sep} = 2010-08-12T05:27:39.114$ (UTC) in terms of mean and covariance, as reported in Table 1. Assume Keplerian motion can be used to model the spacecraft dynamics.

1. Propagate the initial mean and covariance for both satellites within a time grid going from t_{sep} to $t_{sep} + N T_1$, with a step equal to T_1 , where T_1 is the orbital period of satellite 1 and $N = 10$, using both a Linearized Approach (LinCov) and the Unscented Transform (UT). We suggest to use $\alpha = 0.1$ and $\beta = 2$ for tuning the UT in this case.
2. Considering that the two satellites are in close formation, you have to guarantee a sufficient accuracy about the knowledge of their state over time to monitor potential risky situations. For this reason, at each revolution, you shall compute:
 - the norm of the relative position (Δr), and
 - the sum of the two covariances associated to the position elements of the states of the two satellites (P_{sum})

The critical conditions which triggers a collision warning is defined by the following relationship:

$$\Delta r < 3\sqrt{\max(\lambda_i(P_{sum}))}$$

where $\lambda_i(P_{sum})$ are the eigenvalues of P_{sum} . Identify the revolution N_c at which this condition occurs and elaborate on the results and the differences between the two approaches (UT and LinCov).

3. Perform the same uncertainty propagation process on the same time grid using a Monte Carlo (MC) simulation *. Compute the sample mean and sample covariance and compare them with the estimates obtained at Point 1). Provide the plots of:
 - the time evolution for all three approaches (MC, LinCov, and UT) of $3\sqrt{\max(\lambda_i(P_{r,i}))}$ and $3\sqrt{\max(\lambda_i(P_{v,i}))}$, where $i = 1, 2$ is the satellite number and P_r and P_v are the 3x3 position and velocity covariance submatrices.
 - the propagated samples of the MC simulation, together with the mean and covariance obtained with all methods, projected on the orbital plane.

Compare the results and discuss on the validity of the linear and Gaussian assumption for uncertainty propagation.

*Use at least 100 samples drawn from the initial covariance

Table 1: Estimate of Satellite 1 and Satellite 2 states at t_0 provided in ECI J2000.

Parameter	Value
Ref. epoch t_{sep} [UTC]	2010-08-12T05:27:39.114
Mean state $\hat{\mathbf{x}}_{0,sat1}$ [km, km/s]	$\hat{\mathbf{r}}_{0,sat1} = [4622.232026629, 5399.3369588058, -0.0212138165769957]$ $\hat{\mathbf{v}}_{0,sat1} = [0.812221125483763, -0.721512914578826, 7.42665302729053]$
Mean state $\hat{\mathbf{x}}_{0,sat2}$ [km, km/s]	$\hat{\mathbf{r}}_{0,sat2} = [4621.69343340281, 5399.26386352847, -3.09039248714313]$ $\hat{\mathbf{v}}_{0,sat2} = [0.813960847513811, -0.719449862738607, 7.42706066911294]$
Covariance P_0 [km ² , km ² /s, km ² /s ²]	$\begin{bmatrix} +5.6e-7 & +3.5e-7 & -7.1e-8 & 0 & 0 & 0 \\ +3.5e-7 & +9.7e-7 & +7.6e-8 & 0 & 0 & 0 \\ -7.1e-8 & +7.6e-8 & +8.1e-8 & 0 & 0 & 0 \\ 0 & 0 & 0 & +2.8e-11 & 0 & 0 \\ 0 & 0 & 0 & 0 & +2.7e-11 & 0 \\ 0 & 0 & 0 & 0 & 0 & +9.6e-12 \end{bmatrix}$

Point 1

Given the initial states and covariance matrix, the first step is calculating the Mango orbital period. To do so, the Cartesian coordinates need to be transformed into Keplerian parameters. Always in the frame of the *NASA SPICE Toolkit*, the function *cspice_oscltx* is used to achieve this purpose. The function also estimates the orbital period, which is $T_1 = 6004.23$ [s].

For both the Linearized Approach (LinCov) and the Unscented Transform (UT), the equations and procedures seen during lessons are implemented. As for LinCov, the State Transition Matrix (STM) is obtained by applying the variational approach (integrating it alongside the states). Finally, as imposed by the problem statement, the UT parameters are $\alpha = 0.1$, $\beta = 2$ and $k = 0$. Keplerian motion models the spacecraft dynamics.

Point 2

Figure 1 displays the evolution of Δr and the critical distance, $3\sqrt{\max(\lambda_i(P_{sum}))}$, along the satellite revolution. The collision warning is triggered for both approaches at $N_c = 4$ and, looking at the plots, the curves are almost identical for LinCov and UT.

The similarity between these results suggests that the system dynamics are well-approximated by the linear assumption, as it is the same as the one obtained with the Gaussian assumption. The two methods capture the dynamics in the same way and, if there are any differences, they could be caused due to the second-order terms captured by UT. However, to understand if these approaches are indeed appropriately describing the system dynamics, a Monte Carlo (MC) simulation needs to be performed.

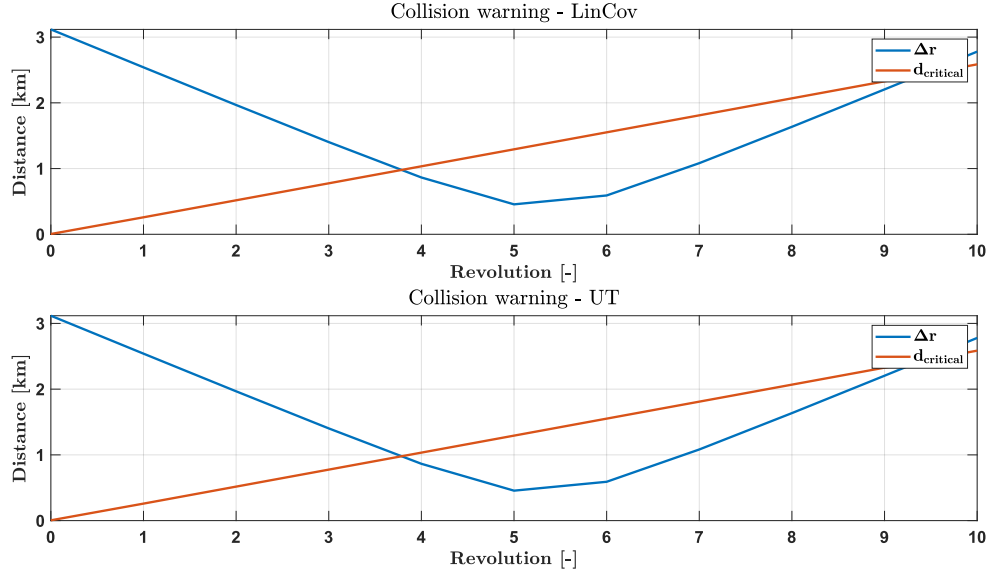
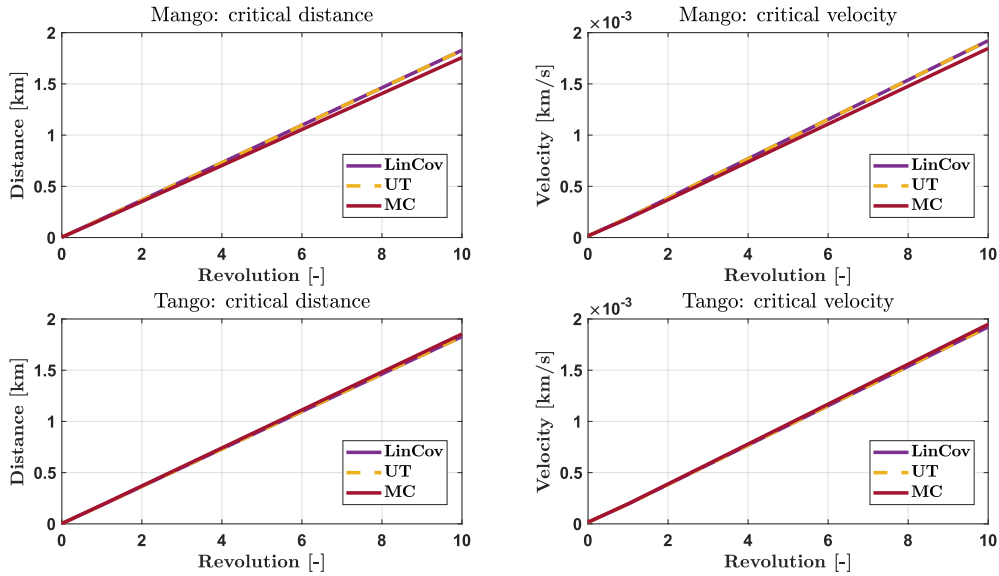


Figure 1: Collision warning trigger

Point 3

Figure 2 shows the evolution of the critical conditions for each satellite using all three propagation methods. For the Monte Carlo simulation, 1000 samples are used. As an initial value, 100 samples were used but this option was discarded as MC strongly relies on this parameter and maybe that number was not enough to capture the behaviour of the system.


 Figure 2: Critical condition analysis - $N_{samp} = 1000$

To project the mean, covariance and MC samples on the orbital plane, the following Local Vertical Local Horizontal (LVLH) frame is selected:

$$\hat{\mathbf{i}} = \frac{\mathbf{r}}{r}, \quad \hat{\mathbf{j}} = \hat{\mathbf{k}} \times \hat{\mathbf{i}}, \quad \hat{\mathbf{k}} = \frac{\mathbf{h}}{h} = \frac{\mathbf{r} \times \mathbf{v}}{\|\mathbf{r} \times \mathbf{v}\|} \quad (1)$$

By concatenating these unit vectors, the rotation matrix to go from ECI to LVLH can be

retrieved for each satellite's initial state and then applied to rotate everything using Equation 2, where R_i is the rotation matrix from ECI to LVLH, $r_{LVLH,i}$ is the position of satellite i in LVLH, $r_{ECI,i}$ is the position of satellite i in ECI and $P_{r,i}$ the position covariance submatrix of satellite i . This analysis is only applied to the position states and covariance submatrices to have better understandable plots and results. This explains why the mean motion of each satellite does not need to be taken into account.

$$r_{LVLH,i} = R_i (r_{ECI,i} - \hat{r}_{0,i}), \quad P_{rLVLH,i} = R_i P_{r,i} R_i^T \quad (\text{for } i = 1, 2) \quad (2)$$

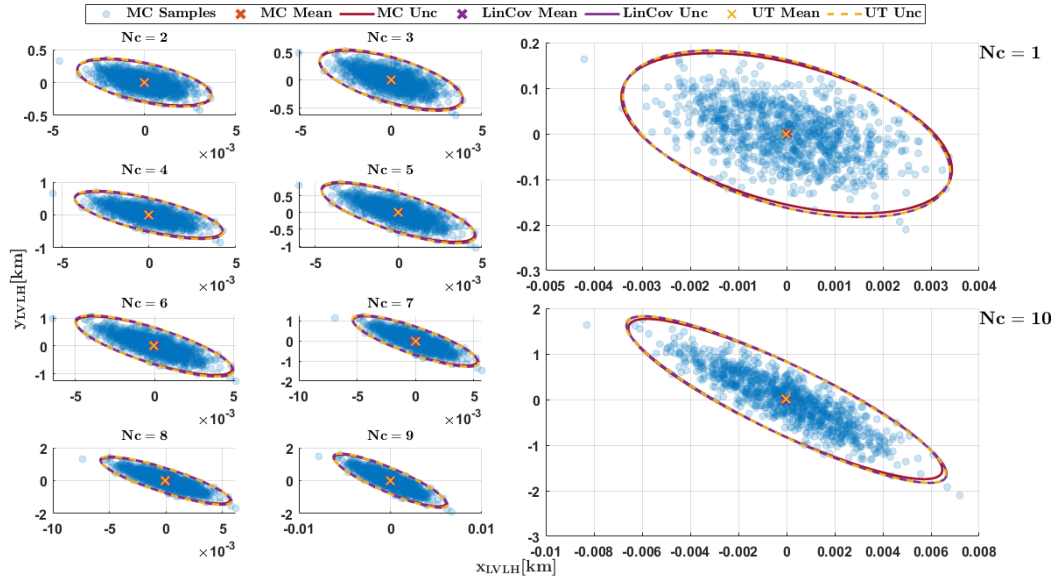


Figure 3: Mango uncertainty analysis in LVLH

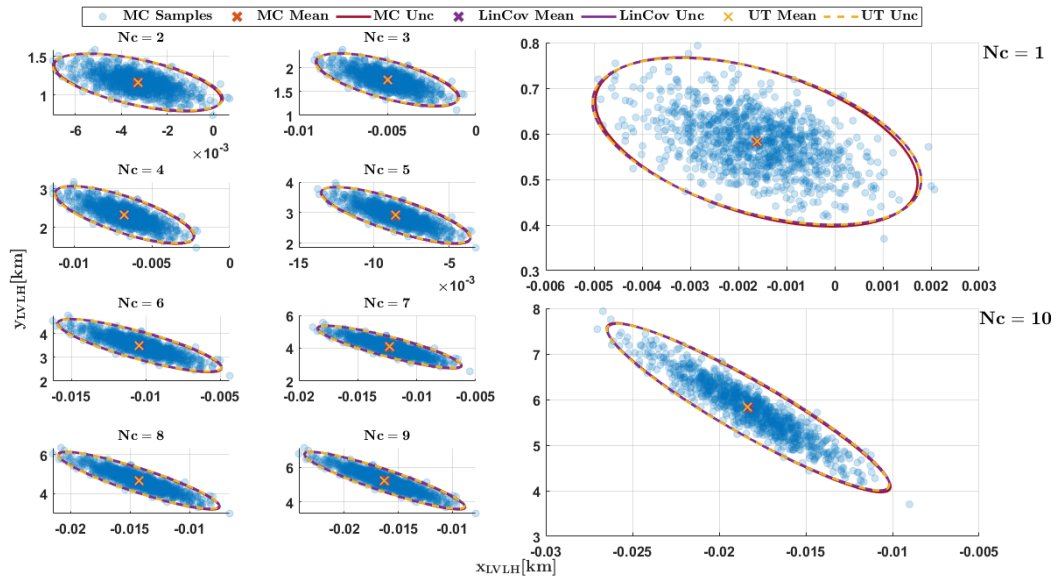


Figure 4: Tango uncertainty analysis in LVLH

In Figures 3 and 4, the parameters specified in the exercise statement are illustrated for Mango and Tango respectively. After the execution of the Monte Carlo analysis, the discussion about the accuracy of the linear and Gaussian assumptions can be resumed. The outcomes



derived using all three methods (LinCov, UT, and Monte Carlo) are notably similar. The similarity between LinCov and UT has been previously discussed. Even though the linear and Gaussian assumptions provide almost identical results, slight variations are observed when these are compared with the Monte Carlo method, which includes the entire spectrum of potential behaviours.

Thus, while the LinCov and UT methods might not perfectly capture the full dynamics of the satellites, the results indicate they adequately model the system, making them suitable for this problem. The appropriateness of these methods is further supported by the inherent nature of Keplerian dynamics. Considering the short duration of the time grid and the nearly circular orbits of the satellites, with an eccentricity nearing zero, a linear approximation of the dynamics seems justified, as evidenced by the results.

Enhancing this analysis could involve increasing the samples in the Monte Carlo simulation. A larger number of samples would lead to more accurate outcomes. However, it is important to note that this would also substantially increase the computational load, which is already considerable with the current simulation of 1000 samples.

Exercise 2: Batch filters

You have been asked to track Mango to improve the accuracy of its state estimate. To this aim, you shall schedule the observations from the two ground stations reported in Table 2.

1. *Compute visibility windows.* By using the mean state reported in Table 1 and by assuming Keplerian motion, predict the trajectory of the satellite over a uniform time grid (with a time step of 60 seconds) and compute all the visibility time windows from the available stations in the time interval from $t_0 = 2010-08-12T05:30:00.000$ (UTC) to $t_f = 2010-08-12T11:00:00.000$ (UTC). Plot the resulting predicted Azimuth and Elevation profiles in the visibility windows.
2. *Simulate measurements.* The Two-Line Elements (TLE) set of Mango are reported in Table 3 (and in WeBeep as 36599.3le). Use SGP4 and the provided TLEs to simulate the measurements acquired by the sensor network in Table 2 by:
 - (a) Computing the spacecraft position over the visibility windows identified in Point 1 and deriving the associated expected measurements.
 - (b) Simulating the measurements by adding a random error to the expected measurements (assume a Gaussian model to generate the random error, with noise provided in Table 2). Discard any measurements (i.e., after applying the noise) that does not fulfill the visibility condition for the considered station.
3. *Solve the navigation problem.* Using the measurements simulated at the previous point:
 - (a) Find the least squares (minimum variance) solution to the navigation problem without a priori information using
 - the epoch t_0 as reference epoch;
 - the reference state as the state derived from the TLE set in Table 3 at the reference epoch;
 - the simulated measurements obtained for the KOROU ground station only;
 - pure Keplerian motion to model the spacecraft dynamics.
 - (b) Repeat step 3a by using all simulated measurements from both ground stations.
 - (c) Repeat step 3b by using J2-perturbed motion to model the spacecraft dynamics.
4. Provide the obtained navigation solutions and elaborate on the results, comparing the different solutions.
5. Select the best combination of dynamical model and ground stations and perform the orbit determination for the other satellite.

Table 2: Sensor network to track Mango and Tango: list of stations, including their features.

Station name	KOUROU	SVALBARD
Coordinates	LAT = 5.25144° LON = -52.80466° ALT = -14.67 m	LAT = 78.229772° LON = 15.407786° ALT = 458 m
Type	Radar (monostatic)	Radar (monostatic)
Provided measurements	Az, El [deg] Range (one-way) [km]	Az, El [deg] Range (one-way) [km]
Measurements noise (diagonal noise matrix R)	$\sigma_{Az,El} = 100$ mdeg $\sigma_{range} = 0.01$ km	$\sigma_{Az,El} = 125$ mdeg $\sigma_{range} = 0.01$ km
Minimum elevation	10 deg	5 deg

Table 3: TLE of Mango.

1_36599U_10028B_10224.22752732_-00000576_00000-0_-16475-3_0_9998
2_36599_098.2803_049.5758_0043871_021.7908_338.5082_14.40871350_8293

Table 4: TLE of Tango.

1_36827U_10028F_10224.22753605_00278492_00000-0_82287-1_0_9996
2_36827_098.2797_049.5751_0044602_022.4408_337.8871_14.40890217_55

Point 1

To retrieve the visibility windows, the following procedure is applied:

- The time grid is created, including as the first point the epoch of the mean state reported in Table 1, which is different from t_0 .
- The initial mean state is propagated using *ode113* assuming Keplerian motion.
- The propagated states are used to retrieve the station-satellite vector in the ground station topocentric frame.
- The relative states are then input in the function *cspice_relat* obtaining range, azimuth and elevation.
- The elevation values are compared with the minimum elevation of the ground station to find the visibility windows.

Following the procedure described above, Figure 5 shows the evolution of the azimuth and elevation profiles over time for each ground station. The initial and final time of each visibility window is also represented by the vertical dashed lines. In total, there are two KOUROU

windows and four SVALBARD windows. Finally, Figure 6 displays the polar graph for each ground station alongside their minimum elevation values.

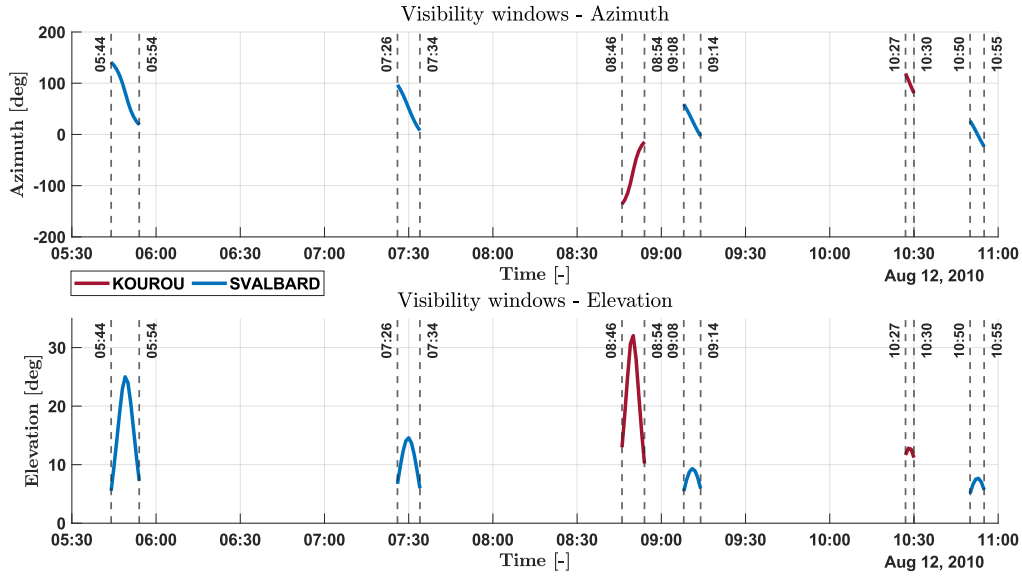


Figure 5: Azimuth and elevation profiles during visibility windows

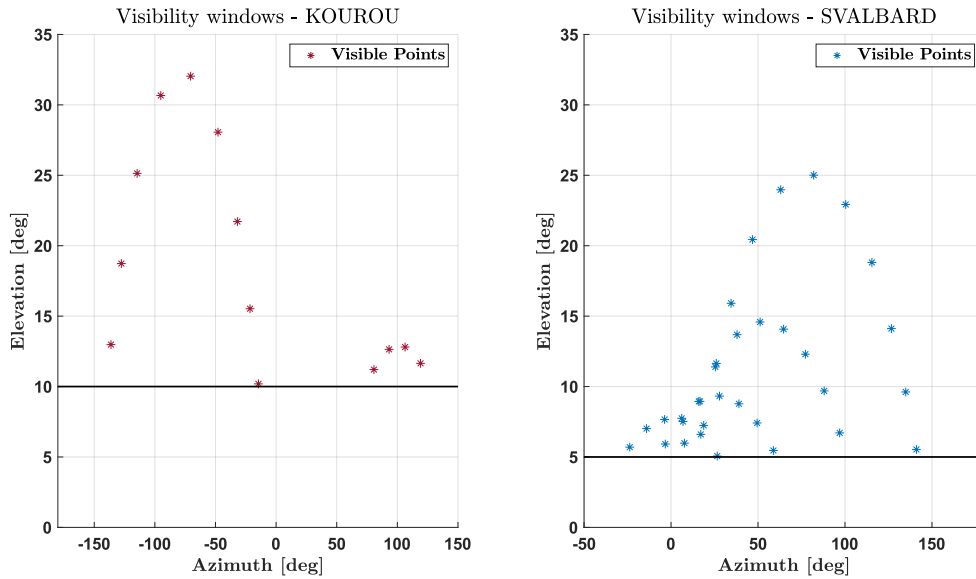


Figure 6: Azimuth vs elevation profile during visibility windows

Point 2

To simulate the measurements, the same procedure as in the previous point is applied but inputting the times inside visibility windows. In this case, the state is propagated using *SGP4* and the conversion from TEME to ECI needs to be taken into account. Then, random noise is included using the *mvrnd* function with the measurements and the ground station noise matrix. Finally, the minimum elevation check is computed again to discard the points outside the visibility range after applying the noise.

Figure 7 shows the simulated measurements' evolution with time. There is a change in the

first KOUROU visibility window, which now lasts one minute less when compared with the previous point results. This is explained by the difference in the propagated dynamics and the addition of noise. The other visibility windows remain the same, even though the measurement values differ from the ones previously estimated.

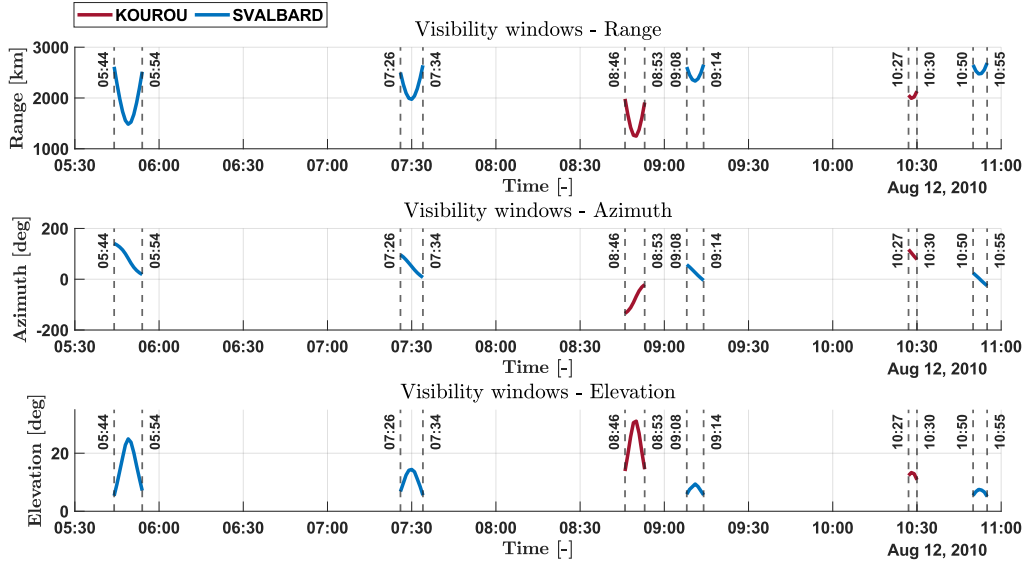


Figure 7: Mango simulated measurements

Points 3 & 4

For the batch filter implementation, the same procedure of Laboratory 04 is followed:

- The initial state guess is propagated for the visibility windows times using the proper dynamical model, either Keplerian or J2-perturbed.
- The predicted measurements are obtained with the same steps explained in Point 1.
- The residuals are then computed by multiplying the weight matrix, derived from the ground station noise matrix, times the difference between real measurements, obtained in the previous Point 2, and predicted ones.
- The residuals are minimized by the *lsqnonlin* function.
- In the case of two ground stations, the framework is the same, but two different propagations are performed, one for each station, and the residuals are then concatenated.

After solving the residuals minimisation problem, the refined state estimation is obtained, and the outputs of the function (jacobian, residuals length and residuals norm) are used to retrieve the covariance matrix associated with the predicted state. The navigation problem solution for each of the cases of the exercise statement, @ Earth ECI, is included in the following equations.

- KOUROU & Keplerian motion (Kep & 1GS):

$$\hat{\mathbf{x}}_0 = \begin{bmatrix} 4665.31 \\ 5255.08 \\ 1015.16 \\ 0.113 \\ -1.491 \\ 7.361 \end{bmatrix}, \quad P = \begin{bmatrix} +5.40e+1 & -1.99e+1 & -1.14e+1 & +4.68e-1 & -9.14e-1 & -2.15e-1 \\ -1.99e+1 & +9.75 & -1.36e+1 & -1.64e-1 & +3.14e-1 & +7.61e-2 \\ -1.14e+1 & -1.36e+1 & +1.64e+2 & -1.72e-1 & +4.86e-1 & +8.82e-2 \\ +4.68e-1 & -1.64e-1 & -1.72e-1 & +4.10e-3 & -8.05e-3 & -1.89e-3 \\ -9.14e-1 & +3.14e-1 & +4.86e-1 & -8.05e-3 & +1.63e-2 & +3.77e-3 \\ -2.15e-1 & +7.61e-2 & +8.82e-2 & -1.89e-3 & +3.77e-3 & +8.77e-4 \end{bmatrix}$$

- KOUROU, SVALBARD & Keplerian motion (Kep & 2GS):

$$\hat{\mathbf{x}}_0 = \begin{bmatrix} 4666.29 \\ 5248.92 \\ 1039.54 \\ 0.092 \\ -1.548 \\ 7.350 \end{bmatrix}, \quad P = \begin{bmatrix} +3.03e-1 & +8.01e-2 & +1.35e-1 & -2.62e-4 & -4.04e-4 & -3.82e-4 \\ +8.01e-2 & +2.39e-1 & -4.94e-2 & -5.16e-5 & -2.87e-4 & -3.10e-4 \\ +1.35e-1 & -4.94e-2 & +1.04e0 & -6.74e-4 & -2.94e-4 & -1.77e-4 \\ -2.62e-4 & -5.16e-5 & -6.74e-4 & +5.99e-7 & +4.67e-7 & +3.75e-7 \\ -4.04e-4 & -2.87e-4 & -2.94e-4 & +4.67e-7 & +8.91e-7 & +7.37e-7 \\ -3.82e-4 & -3.10e-4 & -1.77e-4 & +3.75e-7 & +7.37e-7 & +7.00e-7 \end{bmatrix}$$

- KOUROU, SVALBARD & J2-perturbed motion (J2 & 2GS):

$$\hat{\mathbf{x}}_0 = \begin{bmatrix} 4685.37 \\ 5238.57 \\ 1042.39 \\ 0.082 \\ -1.556 \\ 7.345 \end{bmatrix}, \quad P = \begin{bmatrix} +3.63e-4 & +9.78e-5 & +1.41e-4 & -2.97e-7 & -4.43e-7 & -4.44e-7 \\ +9.78e-5 & +2.75e-4 & -5.89e-5 & -6.56e-8 & -2.92e-7 & -3.44e-7 \\ +1.41e-4 & -5.89e-5 & +1.37e0 & -8.63e-7 & -2.96e-7 & -1.47e-7 \\ -2.97e-7 & -6.56e-8 & -8.63e-7 & +7.28e-10 & +4.92e-10 & +3.99e-10 \\ -4.43e-7 & -2.92e-7 & -2.96e-7 & +4.92e-10 & +8.76e-10 & +7.42e-10 \\ -4.44e-7 & -3.44e-7 & -1.47e-7 & +3.99e-10 & +7.42e-10 & +7.57e-10 \end{bmatrix}$$

Given the predicted state and covariance matrix, the error with respect to the reference state, computed using SGP4, and the uncertainty of the solution are retrieved through Equation 3, where the subindices r and v refer to position and velocity respectively.

$$\epsilon_{r,v} = \text{norm}(\mathbf{r}, \mathbf{v}_{\text{reference}} - \mathbf{r}, \mathbf{v}_{\text{predicted}}), \quad 3\sigma = 3\sqrt{\text{trace}(P_{\text{predicted}})} \quad (3)$$

The least squares method used to solve the navigation problem inherently minimizes a nonlinear problem. This approach can lead to various local minima, depending on the initial estimates. Some of those minima provide solutions where the error falls within the uncertainty bounds, successfully containing the reference state within the ellipsoid. Others, however, may result in larger errors, providing a reference state outside the uncertainty. To understand the nature and capabilities of the batch filter, many different initial guesses are used to find a solution that indeed contains the reference state inside the uncertainty ellipsoid. This involves propagating the Mango state and covariance matrix to the reference time t_0 using LinCov method, and generating random initial estimates until a suitable local minimum is found.

Table 5: Mango navigation problem comparison

Parameter	Kep & 1GS	Kep & 2GS	J2 & 2GS
ϵ_r [km]	37.6396	21.8547	0.0616
$3\sigma_r$ [km]	45.3175	3.7706	0.1344
ϵ_v [km/s]	$7.4183e-2$	$1.4773e-2$	$3.1162e-5$
$3\sigma_v$ [km/s]	$4.3735e-1$	$4.4390e-3$	$1.4576e-4$

The results shown in Table 5 reveal successful solutions only for Keplerian motion with Kourou measurements and J2-perturbed motion with data from both ground stations. These outcomes highlight two key factors influencing the least squares method: the precision of the dynamical model and the real measurements' contribution to refining the initial estimate. The dynamical model primarily affects the error relative to the reference state, while the measurements mainly influence the solution's uncertainty. When the dynamical model deviates significantly from SGP4, such as in Keplerian motion, the error remains substantial, but the limited Kourou measurements result in high uncertainty, allowing the error to fit within 3σ . Conversely, incorporating measurements from two stations reduces uncertainty but does not allow to compensate for the large error given by an imprecise model, leading to inaccurate predictions. Introducing J2 perturbations aligns the model more closely with SGP4, reducing error and enabling the reference state to fall within the uncertainty bounds.

This analysis underscores the batch filter's reliance on three main aspects: the dynamical model's accuracy, measurement accuracy and number, and the initial guess. In real-world applications, however, generating random initial guesses based on the propagated state and covariance is not possible, since the actual reference state is unknown. Even so, this approach is implemented to see if the currently considered cases could provide appropriate solutions depending on the provided initial guesses. This implies the need for an improved dynamical model to obtain a solution that always contains the real reference state using as initial guess the propagated mean state. For instance, including drag forces, modelled by SGP4, can provide a better dynamical model.

Additionally, the combination of J2 dynamics and two ground station measurements is the best approach, and it is then used for Tango implementation.

Point 5

The same procedure used in Points 1, 2, 3 and 4 is now applied to Tango to solve its navigation problem. For the least squares minimisation, the combination of J2-perturbed motion and two ground stations is used, as mentioned above. Finally, the initial guess variation using the propagated state and covariance matrix with LinCov is also implemented to find a solution containing the reference state inside the uncertainty ellipsoid. The navigation problem solution @ Earth ECI, including the error and uncertainty, is introduced hereafter.

$$\hat{\mathbf{x}}_0 = \begin{bmatrix} 4685.13 \\ 5238.80 \\ 1039.61 \\ 0.083 \\ -1.555 \\ 7.345 \end{bmatrix}, \quad P = \begin{bmatrix} +1.80e-2 & +4.64e-3 & +6.84e-3 & -1.46e-5 & -1.93e-5 & -2.10e-5 \\ +4.64e-3 & +1.33e-2 & +1.86e-4 & -4.54e-6 & -1.25e-5 & -1.59e-5 \\ +6.84e-3 & +1.86e-4 & +4.08e-2 & -2.58e-5 & -1.01e-5 & -1.11e-5 \\ -1.46e-5 & -4.54e-6 & -2.58e-5 & +2.61e-8 & +2.02e-8 & +2.09e-8 \\ -1.93e-5 & -1.25e-5 & -1.01e-5 & +2.02e-8 & +3.20e-8 & +3.06e-8 \\ -2.10e-5 & -1.59e-5 & -1.11e-5 & +2.09e-8 & +3.06e-8 & +3.45e-8 \end{bmatrix}$$

Table 6: Tango navigation problem

Parameter	Value
ϵ_r [km]	0.1822
$3\sigma_r$ [km]	$3.0023e-4$
ϵ_v [km/s]	$5.2848e-4$
$3\sigma_v$ [km/s]	$9.1279e-4$

Exercise 3: Sequential filters

According to the Formation Flying In Orbit Ranging Demonstration experiment (FFIORD), PRISMA's primary objectives include testing and validation of GNC hardware, software, and algorithms for autonomous formation flying, proximity operations, and final approach and recede operations. The cornerstone of FFIORD is a Formation Flying Radio Frequency (FFRF) metrology subsystem designed for future outer space formation flying missions.

FFRF subsystem is in charge of the relative positioning of 2 to 4 satellites flying in formation. Each spacecraft produces relative position, velocity and line-of-sight (LOS) of all its companions.

You have been asked to track Mango to improve the accuracy of the estimate of its absolute state and then, according to the objectives of the PRISMA mission, validate the autonomous formation flying navigation operations by estimating the relative state between Mango and Tango by exploiting the relative measurements acquired by the FFRF subsystem. The Two-Line Elements (TLE) set of Mango and Tango satellites are reported in Tables 3 and 4 (and in WeBeep as 36599.3le, and 36827.3le).

The relative motion between the two satellites can be modelled through the linear, Clohessy-Wiltshire (CW) equations[†]

$$\begin{aligned}\ddot{x} &= 3n^2x + 2n\dot{y} \\ \ddot{y} &= -2n\dot{x} \\ \ddot{z} &= -n^2z\end{aligned}\tag{4}$$

where x , y , and z are the relative position components expressed in the LVLH frame, whereas n is the mean motion of Mango, which is assumed to be constant and equal to:

$$n = \sqrt{\frac{GM}{R^3}}\tag{5}$$

where R is the position of Mango at t_0 .

The unit vectors of the LVLH reference frame are defined as follows:

$$\hat{\mathbf{i}} = \frac{\mathbf{r}}{r}, \quad \hat{\mathbf{j}} = \hat{\mathbf{k}} \times \hat{\mathbf{i}}, \quad \hat{\mathbf{k}} = \frac{\mathbf{h}}{h} = \frac{\mathbf{r} \times \mathbf{v}}{\|\mathbf{r} \times \mathbf{v}\|}\tag{6}$$

To perform the requested tasks you should:

1. *Estimate Mango absolute state.* You are asked to develop a sequential filter to narrow down the uncertainty on the knowledge of Mango absolute state vector. To this aim, you shall schedule the observations from the SVALBARD ground station[‡] reported in Table 2, and then proceed with the state estimation procedure by following these steps:
 - (a) By using the mean state reported in Table 1 and by assuming Keplerian motion, predict the trajectory of the satellite over a uniform time grid (with a time step of 5 seconds) and compute the first visibility time window from the SVALBARD station in the time interval from $t_0 = 2010-08-12T05:30:00.000$ (UTC) to $t_f = 2010-08-12T06:30:00.000$ (UTC).
 - (b) Use SGP4 and the provided TLE to simulate the measurements acquired by the SVALBARD station for the Mango satellite only. For doing it, compute the spacecraft position over the visibility window using a time-step of 5 seconds, and derive the associated expected measurements. Finally, simulate the measurements by adding a random error (assume a Gaussian model to generate the random error, with noise provided in Table 2).

[†]Notice that the system is linear, therefore it has an analytic solution of the state transition matrix Φ

[‡]Note that these are the same ones computed in Exercise 2

- (c) Using an Unscented Kalman Filter (UKF), provide an estimate of the spacecraft state (in terms of mean and covariance) by sequentially processing the acquired measurements in chronological order. Plot the time evolution of the error estimate together with the 3σ of the estimated covariance for both position and velocity.
2. *Estimate the relative state.* To validate the formation flying operations, you are also asked to develop a sequential filter to narrow down the uncertainty on the knowledge of the relative state vector. To this aim, you can exploit the relative azimuth, elevation, and range measurements obtained by the FFRF subsystem, whose features are reported in Table 7, and then proceed with the state estimation procedure by following these steps:
- (a) Use SGP4 and the provided TLEs to propagate the states of both satellites at epoch t_0 in order to compute the relative state in LVLH frame at that specific epoch.
- (b) Use the relative state as initial condition to integrate the CW equations over the time grid defined in Point 1a. Finally, simulate the relative measurements acquired by the Mango satellite through its FFRF subsystem by adding a random error to the expected measurements. Assume a Gaussian model to generate the random error, with noise provided in Table 7.
- (c) Consider a time interval of 20 minutes starting from the first epoch after the visibility window (always with a time step of 5 seconds). Use an UKF to provide an estimate of the spacecraft relative state in the LVLH reference frame (in terms of mean and covariance) by sequentially processing the measurements acquired during those time instants in chronological order. Plot the time evolution of the error estimate together with the 3σ of the estimated covariance for both relative position and velocity.
3. *Reconstruct Tango absolute covariance.* Starting from the knowledge of the estimated covariance of the absolute state of Mango, computed in Point 1, and the estimated covariance of the relative state in the LVLH frame, you are asked to provide an estimate of the covariance of the absolute state of Tango. You can perform this operation as follows:
- (a) Pick the estimated covariance of the absolute state of Mango at the last epoch of the visibility window, and propagate it within the time grid defined in Point 2c.
- (b) Rotate the estimated covariance of the relative state from the LVLH reference frame to the ECI one within the same time grid.
- (c) Sum the two to obtain an estimate of the covariance of the absolute state of Tango. Plot the time evolution of the 3σ for both position and velocity and elaborate on the results.

Table 7: Parameters of FFRF.

Parameter	Value
Measurements noise $\sigma_{Az,El} = 1$ deg (diagonal noise matrix R) $\sigma_{range} = 1$ cm	

Point 1

The visibility windows calculation and the measurements simulation are done following the same procedure as in Points 1 and 2 of the previous exercise. The retrieved solutions are the same as the ones already displayed in that exercise increased in accuracy as now the time step is 5 seconds instead of 60. To avoid a repetitive and long report, the visibility windows and measurement simulation plots are not included in this exercise.

Once the real measurements are simulated, the UKF is implemented by following the instructions explained during the lectures:

- The weights and sigma points are retrieved.
- The sigma points are propagated using J2-perturbed motion. This dynamics model has been proven to be closer to SGP4 in the previous exercise and, therefore, is the one selected for the implementation of the UKF.
- The predicted mean state and covariance matrix are retrieved.
- The sigma points are used to estimate the predicted measurements.
- The predicted measurements, states, and their respective mean values and the real measurements are used to retrieve the measurements' covariance and cross-covariance.
- The Kalman gain is computed.
- Finally, the a posteriori mean state and covariance matrix are retrieved.

This process is followed at every time step of the first visibility window to sequentially apply the filter. To retrieve the initial guesses, the Mango state and covariance matrix introduced in Table 1 are propagated to the first point of the visibility window using the Unscented Transform (UT) method to be consistent with the UKF working principle. The parameters selected for both UT and UKF are $\alpha = 1e - 3$, $\beta = 2$ and $k = 0$. Finally, to retrieve the error, the states propagated with SGP4 are used as reference values. The following Equation 7 is applied to calculate both the error, ϵ , and uncertainty, 3σ , where r and v refer to position and velocity respectively.

$$\epsilon_{r,v} = norm(\mathbf{r}, \mathbf{v}_{k-reference} - \mathbf{r}, \mathbf{v}_{k-predicted}^+), \quad 3\sigma = 3\sqrt{trace(P_{k-predicted}^+)} \quad (7)$$

Figure 8 shows the Mango error and uncertainty evolution in every step of the UKF. It is clear how the uncertainty follows a decreasing trend over time. The error follows this trend as well, but it is masked by the noise generated during measurement acquisition. The behaviour of both quantities suggests that the UKF is working correctly. Nevertheless, the initial covariance matrix needs to be scaled with a factor of $1e + 4$ to have a enough wide initial uncertainty. UKF is very sensitive to the initial values as it works by narrowing the error with respect to the reference and the uncertainty. If the initial predicted state is too accurate, the UKF have trouble reducing the error. However, if the initial uncertainty is small, the UKF is capable of reducing it even to lower values. This situation may generate an unwanted scenario in which the real state remains outside the predicted state uncertainty ellipsoid, generating a failed navigation solution.

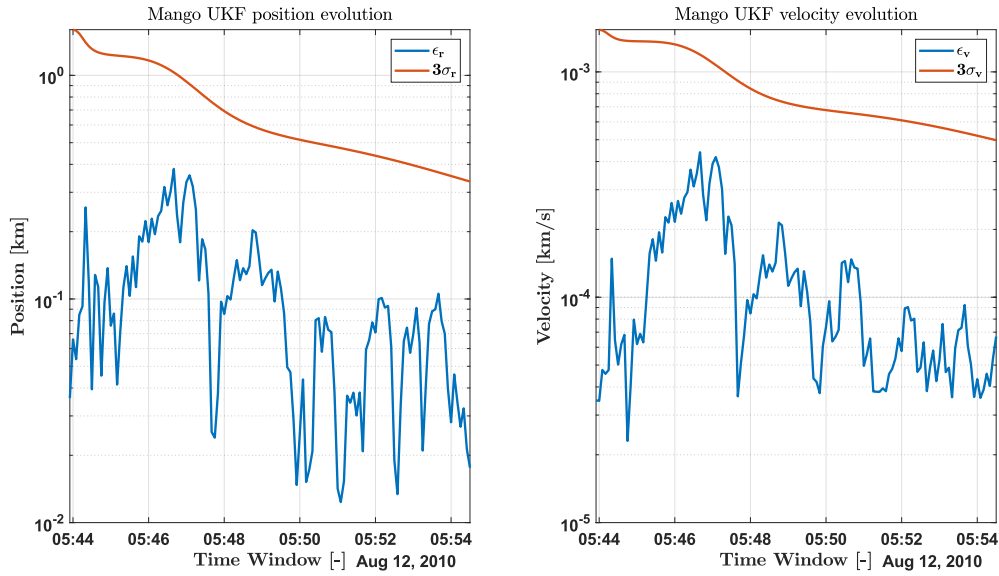


Figure 8: Mango navigation problem solution with UKF

Point 2

Based on the LVLH frame provided by the exercise statement, the rotation matrix to rotate from ECI to LVLH coordinates can be derived. However, as the velocity state and covariance submatrix need to be rotated, the contribution of the rotational motion of the LVLH frame with respect to the ECI one needs to be taken into account. The final rotation matrix is provided in Equation 8, where n is the Mango mean motion parameter, GM the Earth's gravitational constant and r the Mango's position norm.

$$R_{ECI2LVLH} = \begin{bmatrix} R & 0_{3 \times 3} \\ \dot{R} & R \end{bmatrix} \quad \text{where } R = \begin{bmatrix} \hat{i} \\ \hat{j} \\ \hat{k} \end{bmatrix}, \dot{R} = \begin{bmatrix} 0 & -n & 0 \\ n & 0 & 0 \\ 0 & 0 & 0 \end{bmatrix} \quad \text{and } n = \sqrt{\frac{GM}{r^3}} \quad (8)$$

The relative state at t_0 , @ Mango LVLH, $\mathbf{x}_{0,\text{rel}}$, calculated as $R_{ECI2LVLH} \mathbf{x}_{0,\text{rel}} - \mathbf{ECI}$, is:

$$\mathbf{x}_{0,\text{rel}} = (0.4809, -2.9608, 0.0744, -4.9660e-4, 9.8485e-4, -9.1634e-5)^T \quad [\text{km}, \text{km/s}]$$

The same procedure as in Exercise 2 is followed to simulate the measurements. In this case, the FFRF subsystem takes measurements of Tango from Mango, so the relative state between the system and the target is already computed through the LVLH relative state. In this frame, the function *cspice_relat* can be directly applied to retrieve Tango's range, azimuth and elevation. To propagate the state, the analytical solution of the CW equations is exploited as described in Equation 9, where t_0 and \mathbf{x}_0 are the initial time and state, and t_k and \mathbf{x}_k the time and state at step k . By exploiting the dynamics analytical solution, the computational effort is lower when compared with numerical integration.

$$\mathbf{x}_k = \exp[A(t_k - t_0)] \mathbf{x}_0 \quad \text{where } A = \begin{bmatrix} 0 & 0 & 0 & 1 & 0 & 0 \\ 0 & 0 & 0 & 0 & 1 & 0 \\ 0 & 0 & 0 & 0 & 0 & 1 \\ 3n^2 & 0 & 0 & 0 & 2n & 0 \\ 0 & 0 & 0 & -2n & 0 & 0 \\ 0 & 0 & -n^2 & 0 & 0 & 0 \end{bmatrix} \quad (9)$$

Once the initial state and the measurements are retrieved, the UKF can be implemented by applying the same steps as in Point 1 but using the CW dynamics to propagate the sigma points and computing the predicted measurements by directly using the function *cspice_relat* with the propagated sigma points. The initial state is the one previously computed, $\mathbf{x}_{0,rel}$, and, as suggested by the professors, the initial covariance matrix is:

$$P_0 = \text{diag}([0.01, 0.01, 0.1, 0.0001, 0.0001, 0.001])$$

Figure 9 displays the relative navigation problem for Tango using the FFRF subsystem and applying UKF for 20 minutes after the first visibility window. To retrieve the error, the propagated states using CW equations are considered as the reference states. Both the error and the uncertainty, calculated using Equation 7, follow a decreasing trend, suggesting that the UKF has been properly implemented and is working correctly. However, this solution is more sensitive to the simulated measurements, as, depending on the run, the error may get larger than 3σ making the navigation problem fail in retrieving the reference state, even though the trend for both quantities is still decreasing.

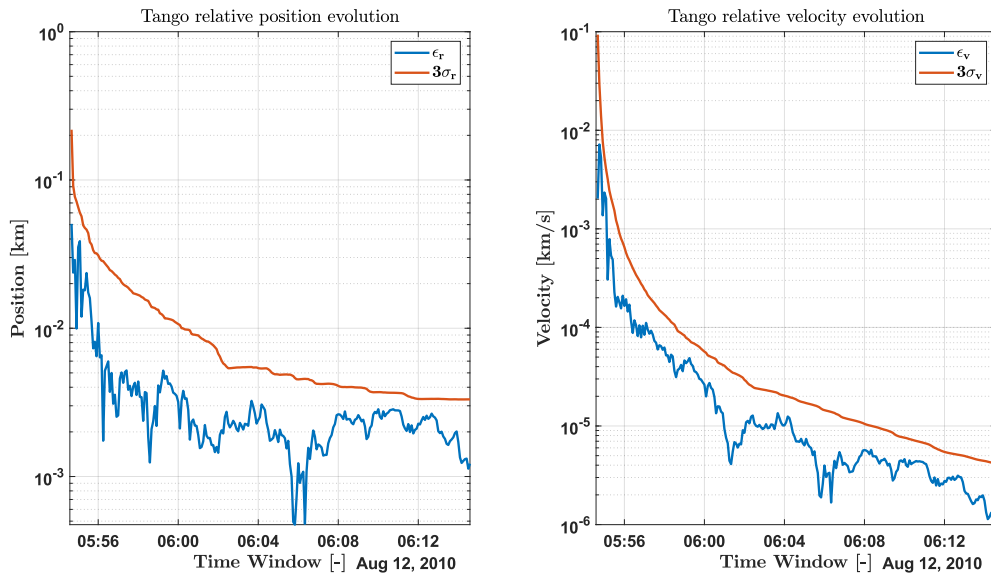


Figure 9: Tango relative navigation problem solution with UKF

Point 3

To retrieve the absolute Tango covariance matrix, the final Mango state and covariance matrix estimated in Point 1 need to be propagated during the same time as Point 2. UT method is the chosen one to do so, as it works with the same principle as the UKF.

Once the propagation is finished, the computed Mango states are used to retrieve the matrix to go from ECI to LVLH as described in Equation 8. This matrix is then employed to rotate the relative Tango covariance matrix as follows. Notice that the transpose is applied in the first matrix as the intention is to go from LVLH to ECI:

$$P_{rel,ECI} = R'_{ECI2LVLH} P_{rel,LVLH} R_{ECI2LVLH}$$

Finally, the absolute Tango covariance matrix is calculated by summing both matrices, the absolute Mango covariance and the relative Tango one. This step can be now performed as they are in ECI frame. To compute the 3σ evolution for both position and velocity, the second part of Equation 7 is applied. The results are introduced in Figure 10 and the trend for both uncertainties is clear, initially, they decrease until they reach a minimum, after which they adopt

a growing behaviour. This is easily explained by the behaviour of both UT, applied to propagate the absolute Mango covariance, and UKF used to estimate the Tango relative covariance matrix. UKF uncertainty, as explained in the previous Points 1 and 2, has a constant decreasing trend while UT, as shown in Exercise 1, increases the uncertainty values through the propagation. As the absolute Tango covariance matrix is calculated using both methods, it combines both trends. Until reaching the minimum, the UKF behaviour dominates, making visible a global decreasing trend, but, from there, the UT takes control over the global effect, and the absolute uncertainty experiences an increasing trend.

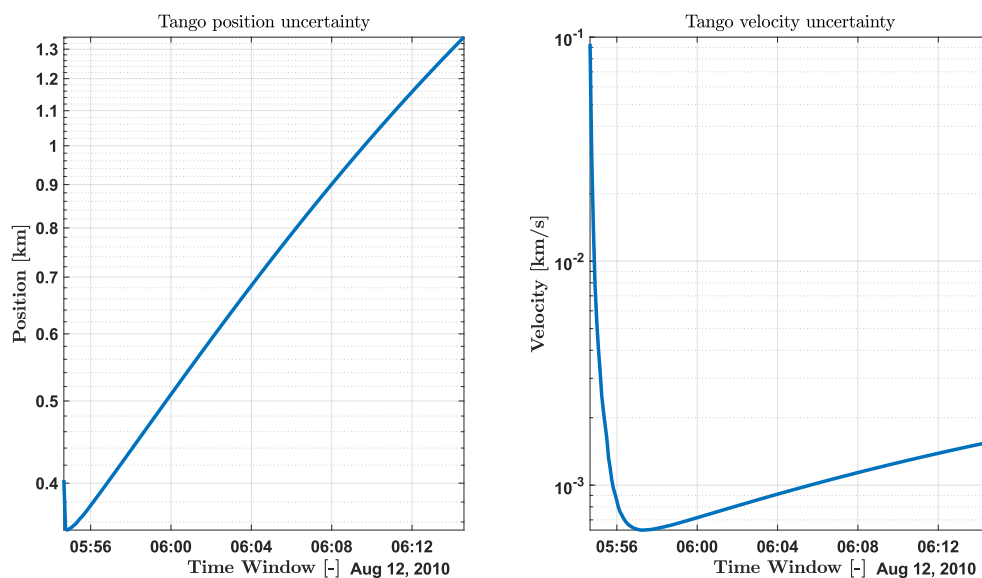


Figure 10: Tango absolute navigation problem solution 3σ evolution